Elasticity-Mediated Self-Organization and Colloidal Interactions of Solid Spheres with Tangential Anchoring in a Nematic Liquid Crystal

I. I. Smalyukh* and O. D. Lavrentovich
Liquid Crystal Institute and Chemical Physics Interdisciplinary Program, Kent State University, Kent, Ohio 44242-0001, USA

A. N. Kuzmin, A. V. Kachynski, and P. N. Prasad
The Institute for Lasers, Photonics, and Biophotonics, University at Buffalo, The State University of New York, Buffalo, New York 14260-3000, USA

(Received 9 June 2005; published 3 October 2005)

Using laser tweezers, we study colloidal interactions of solid microspheres in the nematic bulk caused by elastic distortions around the particles with tangential surface anchoring. The interactions overcome the Brownian motion when the interparticle separation $\vec{\mathbf{r}}_p$ is less than 3 particle diameters. The particles attract when the angle θ between $\vec{\mathbf{r}}_p$ and the uniform far-field director $\hat{\mathbf{n}}_0$ is between 0° and $\approx 70°$ and repel when $75° \lesssim \theta \leq 90°$. The particles aggregate in chains directed at $\approx 30°$ to $\hat{\mathbf{n}}_0$ and, at higher concentrations, form complex kinetically trapped structures.

DOI: 10.1103/PhysRevLett.95.157801 PACS numbers: 61.30.−v, 82.70.Dd, 82.70.Kj, 87.80.Cc

The interaction of particles in the bulk [1–5] and at the surfaces [6] of nematic liquid crystals (LCs) provides a rich variety of new physical phenomena of interest to both the fundamental and applied science of liquid crystals and colloids. The studies recently expanded into the area of optical manipulation of LC colloids [7–9], and to the biological sensors [10]. Anisotropy of molecular interactions at the particle surface leads to elastic distortions of the director $\hat{\mathbf{n}}$. A spherical particle immersed in LC with a uniform far-field director $\hat{\mathbf{n}}_0$ creates distortions that are usually of dipolar or quadrupolar symmetry [1–6]. In the dipolar case, the interactions lead to chaining of particles along $\hat{\mathbf{n}}_0$ [1,4,5,7–9,11] and more complex structures [6,11–14]. Further progress is impossible without a quantitative characterization of the elasticity-mediated forces. Tangentially anchored spheres are of special interest since they are expected to interact as quadrupoles [2,3]. Their interaction has never been characterized quantitatively, although it has been shown that water droplets attract each other along the direction $\theta = 30°$ and eventually coalesce in the nematic LCs [11]. Here we report on the first direct measurement of colloidal interactions for spheres with tangential boundary conditions in the nematic LC. We employ fluorescence confocal polarizing microscopy (FCPM) [15] to characterize the director distortions around the particles and optical trapping with laser tweezers to measure the pair interaction force $\vec{\mathbf{F}}_p$ as a function of the separation $\vec{\mathbf{r}}_p$ between their centers and the angle θ between $\vec{\mathbf{r}}_p$ and $\hat{\mathbf{n}}_0$.

A proper choice of materials is of prime importance for both FCPM and optical tweezer experiments. We use a low birefringence ($\Delta n = 0.04$) nematic ZLI2806 (EM Chemicals) doped with 0.01 wt.% of fluorescent dye *n, n′*-bis(2,5-di-tert-butylphenyl)-3,4,9,10-perylenedicarboximide (BTBP, Aldrich) for FCPM [15]. We use fluorescently labeled Melamine Resin (MR, Aldrich) spheres of diameter $D = 3$ μm. The refractive index of MR ($n = 1.68$) is higher than the average refractive index, $\bar{n} = \sqrt{(2n_0^2 + n_e^2)/3} \approx 1.49$, of ZLI2806 ($n_0$ is the ordinary and n_e the extraordinary refractive indices) to assure stable trapping [9]. The beads were coated with polyisoprene to produce tangentially degenerate alignment with a vanishing azimuthal anchoring coefficient $W_a \lesssim 10^{-10}$ J/m^2 and polar anchoring coefficient $W_p = (0.6 \pm 0.4) \times 10^{-4}$ J/m^2 [16]. The cells are formed by thin (0.15 mm) glass plates; the cell gap $h = (30$–$100)$ μm is set by mylar spacers. Thin polyimide layers (PI2555, HD MicroSystems) at the inner surfaces of the plates are rubbed to set a uniform in-plane $\hat{\mathbf{n}}_0$.

We use a fast version of FCPM based on a Nipkow-disk confocal system integrated with the Nikon microscope Eclipse E-600. We determine the director configurations (through polarization-dependent fluorescence of BTBP) as well as the positions of particles (through fluorescence of rhodamine-B labeling the MR spheres) [9]. We use an optical manipulator (Solar-TII, LM-2) and a laser ($\lambda =$ 1064 nm, power $P = 0$–200 mW) for the dual-beam laser trapping [9]. The optical trap is formed by a 100× objective (NA = 1.3) [17]. Quantitative measurements of forces in LCs require some additional care for three reasons: (1) the difference in refractive indices of the particle and the host depends on the local $\hat{\mathbf{n}}$, (2) the focused light beam can reorient $\hat{\mathbf{n}}$ [8], and (3) light defocusing in a birefringent medium can widen the laser trap [9]. We mitigated these problems by using a low-birefringent LC and particles larger than the waist of the beam (≈ 0.8 μm) [9].

Isolated spheres with tangential anchoring create distortions of the quadrupolar type that quickly decay with distance r from the center of the particle and become optically undetectable at $r \gtrsim 2D$, Fig. 1(a). The director tangential to the sphere forms two point defects—boojums at the poles of particles [18]. When the beads are free to

move around, they attract and form chains oriented at $\theta \approx \pm(25°–35°)$ with respect to $\hat{\mathbf{n}}_0$, Figs. 1(b) and 1(c). The chains elongate with time as other beads join. To verify whether the result is not an artifact of the possible tilt of the chain with respect to the cell plane, we used FCPM observations of the vertical cross sections of thick samples with chains well separated from the bounding plates, Fig. 1(d). FCPM shows that the aggregation angle is indeed $\theta \approx \pm(25°–35°)$, with most of the particles joined at $\theta \approx \pm 30°$. The same angle is observed not only in ZLI2806 with nearly equal splay K_1 and bend K_3 elastic constants, but also in pentylcyanobiphenyl (5CB) with $K_3/K_1 \approx 1.56$, in the mixtures E7 with $K_3/K_1 \approx 1.5$, and ZLI3412 with $K_3/K_1 \approx 1.1$; droplet attraction at $\theta \approx 30°$ has been also reported by Poulin and Weitz [11].

The chains in the bulk can glide on conical surfaces with the apex angle $2\theta \approx 60°$, Figs. 1(e) and 1(f). If the concentration of particles is sufficient, the chains interact and form more complex structures, Figs. 1(e) and 1(f). Chain aggregation results in kinetic trapping (jamming) of particles, similar to the case of isotropic colloids [19,20] but different in the sense that the structures in LC reflect the anisotropy of interactions, Fig. 1(e). Unless the sample is heated to the isotropic phase, the jammed structures do not break apart for months.

To characterize the pair interaction, we used a dual-beam laser trap. Two particles are trapped at different locations and then released by switching off the laser. Their motion is strongly influenced by Brownian motion when r_p is large [pair 1 in Fig. 2(a)], but the anisotropic colloidal interactions become noticeable at $r_p \lesssim (3–4)D$. The particles attract if $0° \leq \theta \lesssim 70°$ and repel if $75° \lesssim \theta \leq 90°$ [pair 2 in Fig. 2(a)]. The attracting particles eventually touch at $\theta \approx 30°$; the particles in the θ range of repulsion continue to undergo fluctuations until they enter the zone of attraction. We further probe the pair interactions by releasing only one bead from the trap while keeping the second trapped; the original separation is kept constant, $r_p = 7.5\ \mu$m, Fig. 2(b). The drift of the particles reflects the direction of interaction force.

To get a better insight into the pattern of repulsive/attractive forces, we perform an experiment in which the position of one particle is fixed by a strong trap ($P = 100$ mW) and the second particle is slowly ($\sim \mu$m/s) moved around it by a low-intensity trap ($P_{\text{lit}} < 5$ mW), Fig. 3. The second trap follows a circle of radius r_t centered at the first trap. The colloidal interactions make the actual separation r_p of the particles different from r_t: $r_p < r_t$ when the particles attract and $r_p > r_t$ when they repel. For relatively large distances, $r_t > 2D$, the strongest attraction is observed at $\theta = 35°–45°$, Figs. 2(a) and 3, which is higher than the aggregation angle $\theta \approx 30°$.

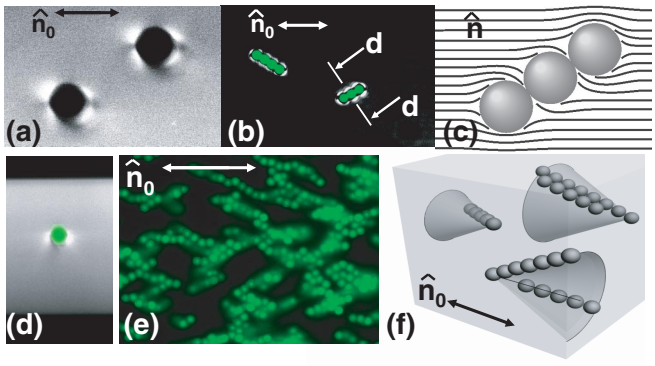

FIG. 1 (color). Colloidal aggregation in the nematic bulk: (a) FCPM texture of the director distortions around a pair of particles; (b) FCPM image of director distortions in the LC colocalized with the fluorescence signal from particles (green) forming chains at $\theta \approx 30°$ to $\hat{\mathbf{n}}_0$; (c) scheme of the director distortions around the spheres in chains; (d) FCPM vertical cross sections along the d-d line in (b) illustrating that the particle chains (green, fluorescence from rhodamine-B) are located in the bulk of LC (gray scale, BTBP); (e) aggregation of spheres leading to kinetically trapped network that reflects anisotropy of the host even at high particle concentration ≈ 5 wt. %; (f) scheme of chain orientations. The FCPM polarization is perpendicular to $\hat{\mathbf{n}}_0$ in (a),(b) and along the chain in (d).

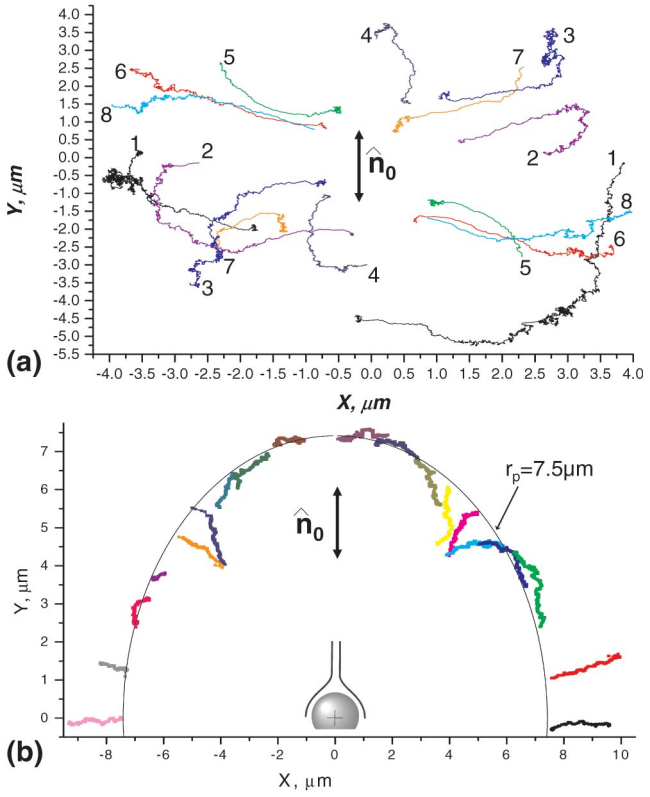

FIG. 2 (color). Trajectories of particle pairs in the LC: (a) both particles are released from the optical traps at different locations (labeled by pairs of numbers 1 through 8; the trajectories of the two particles released at the same time are marked by the same color); (b) one particle is fixed and the other is released from a semicircle of radius $r_p \approx 7.5\ \mu$m at different θ.

To determine $\vec{\mathbf{F}}_p$ we first calibrate stiffness α of the optical trap for different laser powers P [21]. We measure the displacement Δl_d of the trapped bead from its equilibrium position in response to the viscous drag force $F_d = 3\pi D \eta_{\|\mathrm{eff}} V$ as the particle is moved at a constant speed $\vec{V} \| \hat{\mathbf{n}}_0$ in the LC with effective viscosity $\eta_{\|\mathrm{eff}} = 5.9 \times 10^{-5}$ Pa s [22]; the trap stiffness is $\alpha(P) = F_d/\Delta l_d(P)$. The amplitude of $\vec{\mathbf{F}}_p$ is then determined by the displacement Δl_p caused by the pair interaction, $F_p = \alpha \Delta l_p$ [21]. We also use the technique of particle escape to probe interactions at $r_p > 1.5D$ [7,9]. A single particle is moved by the tweezers with an increasing velocity $\vec{V} \| \hat{\mathbf{n}}_0$ until it escapes from the trap at which moment the "trap escape" force is determined by the Stoke's law, $F_{\mathrm{te}} = 3\pi D \eta_{\|\mathrm{eff}} V$. F_{te} is found to be a linear function of P, indicating that nonlinear light-induced processes (such as realignment of $\hat{\mathbf{n}}$ by the laser beam [8]) are insignificant [17]. F_p is measured as F_{te} when the escape from the trap is caused by the pair interaction [7,9]. The results obtained by the two methods above are in a good agreement. The advantage of both approaches is that the effects of anisotropic viscosity of LC are avoided (the velocities of the beads during measurement of F_p are negligibly small) and that both α and F_{te} are practically independent of $\hat{\mathbf{n}}$ around the beads (Δn is small).

To collect the data in Fig. 4, the particles are placed at positions with different θ's but constant r_p, and the force is determined by measuring Δl_p. When the laser power P is reduced, the direction of bead displacement (determined from the optical microscope images) indicates the direction of $\vec{\mathbf{F}}_p$. Figure 4(b) shows how the angle γ between $\vec{\mathbf{r}}_p$ and $\vec{\mathbf{F}}_p$ changes when one particle circumnavigates the other. We measured the distance dependence of $\vec{\mathbf{F}}_p(r_p)$ for $\theta = 30° = \mathrm{const}$, Fig. 5. At $r_p \gtrsim 1.5D$, the dependence $F_p(r_p)$ is close to a power law $\propto r_p^{-6}$, i.e., it is much sharper than in the case of spheres with dipolar distortions of $\hat{\mathbf{n}}$ [5,12]. The force amplitude is of the order of K for $r_p < 2D$ ($K \approx 15$ pN for ZLI2806). In addition to the experiments with $D = 3$ μm, we measured the forces for larger particles, $D = (4\text{–}7.5)$ μm. The qualitative picture remains the same, but $\vec{\mathbf{F}}_p$ increases with D; for example, $\vec{\mathbf{F}}_p$ increases by $\approx 40\%$ when D increases from 3 to 4 μm.

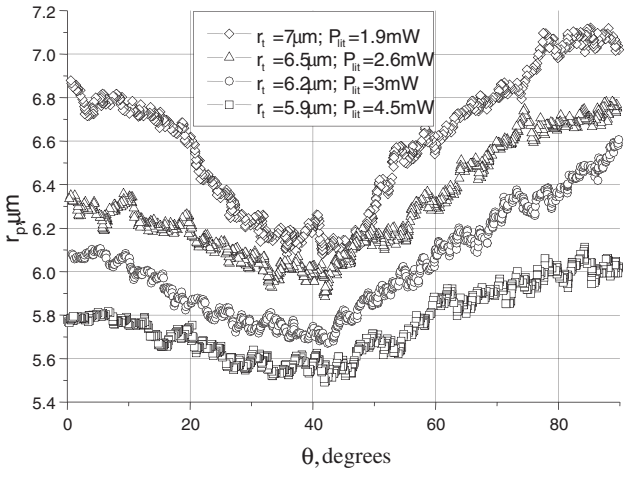

FIG. 3. Angular dependence of the center-to-center distance r_p between two particles measured when one trap moves around the other trap along a circle of a radius r_t.

Let us compare the experimental $\vec{\mathbf{F}}_p(\theta, r_p)$ to available theoretical models for quadrupolar interactions with the pair potential derived for $K_1 = K_3 = K$ [2]:

$$U_q = \frac{\pi W_p^2 R^8}{30 K r_p^5}\left(1 - \frac{W_p R}{56K}\right)(9 + 20\cos 2\theta + 35\cos 4\theta), \tag{1}$$

where $R = D/2$. In Fig. 4 we plot the theoretical predictions for $\vec{\mathbf{F}}_p(\theta, r_p = 1.5D)$ and the θ dependence of the angle γ between $\vec{\mathbf{r}}_p$ and $\vec{\mathbf{F}}_p = -\nabla U_q$ as calculated using

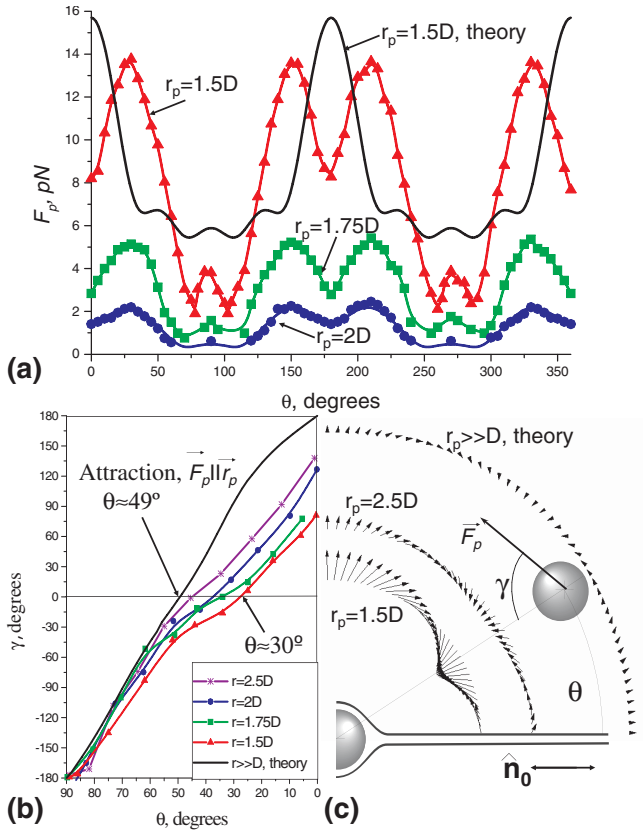

FIG. 4 (color online). Angular dependencies of $\vec{\mathbf{F}}_p$ for two MR particles in the LC: (a) $F_p(\theta)$ measured for $r_p = 1.5D$ (triangles), $r_p = 1.75D$ (squares), and $r_p = 2D$ (circles); (b) the angle γ between $\vec{\mathbf{F}}_p(\theta)$ and $\vec{\mathbf{r}}_p$ as a function of θ; (c) vector representation of $\vec{\mathbf{F}}_p$ as determined experimentally for $r_p = 1.5D$ and $r_p = 2.5D$ and calculated for $r_p \gg D$ using (1).

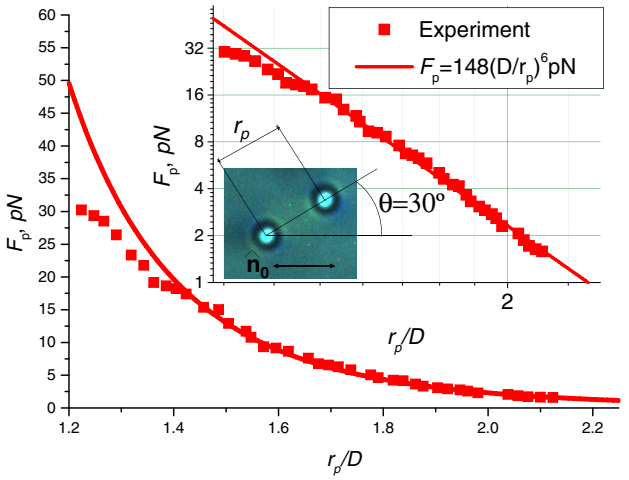

FIG. 5 (color online). F_p vs r_p measured for $\theta \approx 30°$. The solid lines are plots of $F_p = 148(D/r_p)^6$ pN. The inset is the log-log plot of the same data.

Eq. (1) with $K = 15$ pN and $W_p = 5 \times 10^{-5}$ J/m^2; the calculated force is of the same order as in the experiment. The model predicts maximum attraction at $\theta \approx 49°$ which is independent of r_p, while the experiment shows maximum attraction at $\theta \approx 30°$ for $D < r_p < 1.7D$ and at $\theta \approx 35°$–$45°$ for $2D < r_p < 4D$. Furthermore, the experimental repulsive sector is limited to $75° \lesssim \theta \leq 90°$, while the model predicts repulsion also for $\theta \approx 0$. The model dependence $F_p \propto r_p^{-6}$ holds only for $r_p > 1.5D$; at smaller distances it is much weaker, Fig. 5. The discrepancies are not surprising as the model [2,3] assumes $r_p \gg D$ and weak surface anchoring, $K/W_p \gg D$. In the experiment, the elasticity mediated forces overcome the background Brownian motion only when $r_p < (3$–$4)D$; besides, $K/W_p \approx 0.2$ μm, smaller than D. Note that as r_p/D increases, the agreement between the experiment and the model [2,3] improves, Figs. 2–5. To describe the interactions at close separation, the theory should take into account finite surface anchoring and possible deviations of the director from the quadrupolar to lower symmetries.

To conclude, we characterized the pair interaction of colloidal spheres in the nematic host that induce quadrupolar director distortions when isolated. The interactions deviate from the quadrupolar model because the experimental forces are significant only for small interparticle distances. When the concentration of particles increases, they aggregate, first in chains tilted with respect to the far-field director and then into more complex aggregates. The chains break apart once the LC is heated to the isotropic phase (provided that the beads are charge stabilized); the system, therefore, is of interest to study kinetic arrest and jamming [19] in anisotropic media with both attractive and repulsive interactions [20].

We thank B. Senyuk, S. Shiyanovskii, and H. Stark for discussions. We acknowledge support of the NSF Grant No. DMR-0315523 (Kent) and the AFOSR DURINT Grant No. F496200110358 (SUNY). I. I. S. acknowledges support of the Institute for Complex and Adaptive Matter.

*Electronic address: smalyukh@lci.kent.edu

[1] P. Poulin, H. Stark, T. C. Lubensky, and D. A. Weitz, Science **275**, 1770 (1997).
[2] R. W. Ruhwandl and E. M. Terentjev, Phys. Rev. E **55**, 2958 (1997).
[3] S. Ramaswamy, R. Nityananda, V. Raghunathan, and J. Prost, MCLC **288**, 175 (1996).
[4] J. I. Fukuda, H. Stark, M. Yoneya, and H. Yokoyama, Phys. Rev. E **69**, 041706 (2004).
[5] H. Stark, Phys. Rep. **351**, 387 (2001).
[6] I. I. Smalyukh *et al.*, Phys. Rev. Lett. **93**, 117801 (2004).
[7] M. Yada, J. Yamamoto, and H. Yokoyama, Phys. Rev. Lett. **92**, 185501 (2004).
[8] I. Muševič *et al.*, Phys. Rev. Lett. **93**, 187801 (2004).
[9] I. Smalyukh *et al.*, Appl. Phys. Lett. **86**, 021913 (2005).
[10] V. K. Gupta *et al.*, Science **279**, 2077 (1998); S. V Shiyanovskii *et al.*, Phys. Rev. E **71**, 020702(R) (2005).
[11] P. Poulin and D. A. Weitz, Phys. Rev. E **57**, 626 (1998).
[12] P. Poulin, V. Cabuil, and D. A. Weitz, Phys. Rev. Lett. **79**, 4862 (1997).
[13] J. I. Fukuda and H. Yokoyama, Phys. Rev. Lett. **94**, 148301 (2005).
[14] J. Loudet *et al.*, Langmuir **20**, 11 336 (2004).
[15] I. I. Smalyukh, S. V. Shiyanovskii, and O. D. Lavrentovich, Chem. Phys. Lett. **336**, 88 (2001).
[16] I. I. Smalyukh and O. D. Lavrentovich, Phys. Rev. Lett. **90**, 085503 (2003).
[17] P. N. Prasad, *Introduction to Biophotonics* (Wiley, New York, 2003).
[18] M. Kleman and O. D. Lavrentovich, *Soft Matter Physics: An Introduction* (Springer-Verlag, New York, 2003).
[19] V. Trappe, V. Prasad, L. Cipelletti, P. Segre, and D. A. Weitz, Nature (London) **411**, 772 (2001).
[20] A. I. Campbell, V. J. Anderson, J. S. van Duijneveldt, and P. Bartlett, Phys. Rev. Lett. **94**, 208301 (2005).
[21] K. C. Neuman and S. M. Block, Rev. Sci. Instrum. **75**, 2787 (2004).
[22] $\eta_{\|\text{eff}}$ is determined from the Stokes-Einstein relation $\eta_{\|\text{eff}} = k_B T/3\pi\delta_{\|} D$, where k_B is the Boltzmann constant, T is temperature, and $\delta_{\|}$ is the diffusion coefficient measured by analyzing Brownian motion of the bead, as described in Ref. [23].
[23] J. Loudet, P. Hanusse, and P. Poulin, Science **306**, 1525 (2004).